

## **THERMAL BEHAVIOUR AND VIBRATIONAL CHARACTERIZATION OF $MH_2(IO_3)_3$ PHASES ( $M = K, Rb$ and $NH_4$ )**

*M. B. Vassallo and I. L. Botto*

QUIMICA INORGANICA, FACULTAD DE CIENCIAS EXACTAS, UNIVERSIDAD NACIONAL DE LA PLATA, LA PLATA 1900, ARGENTINA

The thermal behaviour of the  $MH_2(IO_3)_3$  ( $M = K, Rb$  and  $NH_4$ ) isomorphous compounds, as well as the IR and Raman spectra have been investigated as part of a study of the properties of solid protonic conductors. Detailed stoichiometries, sustained by TG, DTA, XRD and IR analysis, have been developed into the three phases. There were also evidences of the formation of the  $[I_3O_8]^-$  polymeric phases. Their stabilities were associated to the different polarizing power of the H, K and Rb cations.

**Keywords:** isomorphous compounds, solid protonic conductors, TG, DTA, XRD, IR

### **Introduction**

The solid protonic conductors, which are materials used for electrode and fuel cells, have lately led to a lot of investigations. The structural, thermal and spectroscopic characterization of these phases are undoubtedly related to the protonic mobility.

The ammonium diacid iodate  $(NH_4)H_2(IO_3)_3$  has been found to exhibit protonic conductivity [1]. Although the literature provides general information about the  $MH_2(IO_3)_3$  phases ( $M = K, Rb$  and  $NH_4$ ) this is not clear enough [2-9] and the crystal structure of the ammonium and potassium isomorphous salts have been recently analyzed and compared [10]. The present inform attempts to clarify some aspects of these systems. Thus, the thermal and vibrational behaviour of this series have been reported.

## Experimental

The monovalent (ammonium, potassium and rubidium) diacid iodates were obtained by evaporating aqueous solution of  $I_2O_5$  and respective  $MHCO_3$  in dilute sulfuric acid. Small crystals were used as seeds to obtain large crystals by evaporating the solutions.

Powder diffraction data were obtained with a Philips PW 1730 diffractometer, using  $CuK\alpha$  radiation (nickel filter).

IR spectra were recorded with a Perkin Elmer 580-B Spectrophotometer using the CsCl-pellet as well as the nujol technique.

Raman spectra were obtained with a Spex-Ramalog 1403 double monochromator spectrometer, equipped with a SCAMP data processor. The 514.5 nm line of an Ar-ion laser was used for exciting the samples.

The TG and DTA thermal analysis were carried out using a Rigaku CN 8002 L2 thermoanalyzer. The measurements were performed under a  $N_2$  stream ( $0.4 \text{ l}\cdot\text{min}^{-1}$ ). The temperature was raised up to  $700^\circ\text{C}$  (heating rate  $10 \text{ deg}\cdot\text{min}^{-1}$ ). The specimens were analyzed against  $\alpha\text{-Al}_2\text{O}_3$  as reference. Additional thermal studies were carried out in a crucible furnace. The samples were investigated by X-ray diffractometry and IR spectroscopy.

## Results and discussion

According to the X-ray and neutron diffraction studies, the potassium, rubidium and ammonium diacid iodates are isomorphous phases. They belong to the triclinic system, space group  $P1$  and  $Z = 2$ . More recent cell parameters data are shown in Table 1. Although the literature data are not entirely consistent [10], these lattices are structurally built up by a framework of strongly distorted  $IO_6$  octahedra (three I-O bonds are close to  $1.8 \text{ \AA}$  while the other three are farther away at  $2.7 \text{ \AA}$ ) [7, 10]. The polyhedra are linked together by corner sharing and by H-bonds in the ammonium compounds. On the other hand, there are I-O...(H) and I-O...(M) bonds in the remaining K- and Rb-isomorphous phases. The  $NH_4$  and K cations should be considered in a ten coordination [10]. On the other hand, there are three types of slightly different  $IO_6$  polyhedra in the lattice with one common corner and a very complex and highly condensed structural group. Two of these groups are linked in a block of six octahedra, repeated along the three crystallographic axis. This type of framework generates cavities (occupied by the M ions) and also channels running along the three axis of the triclinic lattice, in which the acids protons are located [10]. These H-atoms can easily be removed when an electric field is applied and their migration is responsible for the ionic conductivity. The transversal dimensions of the channels are shorter in  $KH_2(IO_3)_3$  than in the ammonium compound. So, the movement of the protons in-

side the channels is lower in the K phase. Likewise, as the ammonium ion is not very different in size from the Rb ion [11], the XRD patterns for both compounds are similar. Only a very slight shift of the diffraction lines to smaller angles is observed in the last compound.

**Table 1** Cell parameters of  $M\text{H}_2(\text{IO}_3)_3$  ( $M = \text{K}, \text{NH}_4, \text{Rb}$ )

	$\text{KH}_2(\text{IO}_3)_3$ [10]	$\text{NH}_4\text{H}_2(\text{IO}_3)_3$ [10]	$\text{RbH}_2(\text{IO}_3)_3$ [7]
a (Å)	8.266	8.396	8.332
b (Å)	8.200	8.363	8.232
c (Å)	8.180	8.207	8.264
$\alpha$ (°)	66.08	65.57	60.66
$\beta$ (°)	60.16	60.13	85.80
$\gamma$ (°)	71.06	70.33	66.10

Finally, comparing the ammonium and potassium structural information, it is possible to get the following conclusions:

- i) In the framework, there are three shorter I–O distances.
- ii) The I–O...(K) bond-length is increased in relation to the I–O...(NH<sub>4</sub>) one.
- iii) The shortening of the I–O...(H<sub>prot</sub>) bond is more evident in the case of the K phase. Therefore, a lengthening of the O–H<sub>prot</sub> distance is observed in this case.
- (iv) Finally, the shortest H<sub>prot</sub>–H<sub>prot</sub> distance (into the channels) is observed in the K phase.

### *Vibrational behaviour*

The IR and Raman spectra of the ammonium and potassium compounds were recently published by Santha *et al.* [12]. However, whereas the Raman lines agree with our results, the IR spectra show differences. This discrepancy is attributed to the fact that the samples were prepared using the KBr pellet technique. As it is known, under these conditions an immediate redox reaction, between the iodate acid and the Br<sup>−</sup> ions takes place, which alters the original composition of the sample. This observation has been experimented in our laboratory and for this reason the vibrational behaviour of all members of the series has been analyzed in CsCl as well as in nujol [13, 14].

Figure 1 shows a typical vibrational spectrum of the (NH<sub>4</sub>)H<sub>2</sub>(IO<sub>3</sub>)<sub>3</sub> phase, registered between 1300–200 cm<sup>−1</sup>. Four fundamental vibrational frequencies, all IR and Raman active, are to be expected for IO<sub>3</sub>(C<sub>3v</sub>) pyramidal symmetry:  $\nu_1$  (symmetric stretching) at 780 cm<sup>−1</sup>,  $\nu_2$  (symmetric bending) at 390 cm<sup>−1</sup>,  $\nu_3$  (antisymmetric stretching) at 830 cm<sup>−1</sup> and the  $\nu_4$  (antisymmetric bending) at 330 cm<sup>−1</sup> [15, 16]. Likewise, it is usual that the 2 $\nu_2$  symmetric bending overtone,

appears in the Raman effect in the stretching region ( $700\text{--}800\text{ cm}^{-1}$ ) and its intensity can be amplified by Fermi resonance with the  $\nu_1$  symmetric mode. Thus it is difficult to assign the spectra correctly because, although the strongest IR bands can be attributed to the  $\nu_3$  components, it is not so clear to distinguish between  $2\nu_2$  and  $\nu_1$  modes in the Raman effect [17].

On the other hand, the I-O-H vibrations are usually observed in the  $1300\text{--}1100\text{ cm}^{-1}$  region ( $\delta$  I-O-H), as well as near  $650\text{ cm}^{-1}$  ( $\nu$  I-O-(H)) [18]. In the first region, the  $\delta$  I-O-H vibration is splitted and located at higher frequencies than those observed for the free iodic acid [19]. This can be explained by the increase of the I-O-H angle, similar to that found in  $\text{BeH}_2(\text{IO}_3)_3 \cdot 6\text{H}_2\text{O}$  [20].

Table 2 gives the frequencies of the vibrational spectra of the  $\text{MH}_2(\text{IO}_3)_3$  ( $M = \text{K}, \text{Rb}$  and  $\text{NH}_4$ ) phases. The assignment has been done on the basis of very distorted and condensed  $\text{IO}_3$  groups. It is clear that the ammonium and rubidium

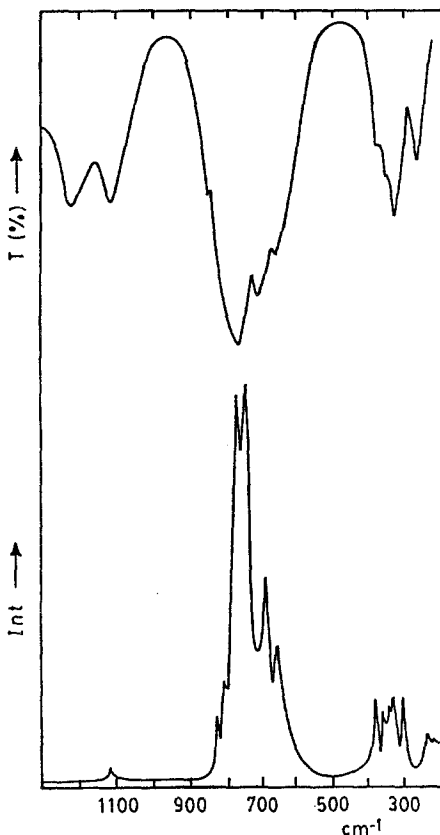


Fig. 1 Vibrational spectrum of  $(\text{NH}_4)\text{H}_2(\text{IO}_3)_3$  (between  $1300\text{--}200\text{ cm}^{-1}$ ) Top: IR; bottom: Raman

spectra show similar and comparable values, fundamentally for the I-O...*M* stretching modes, but they are located at higher frequencies than the corresponding to the  $\text{KH}_2(\text{IO}_3)_3$  spectrum.

### Thermal behaviour

The TG and DTA traces recorded in typical experiments for  $\text{MH}_2(\text{IO}_3)_3$  (*M* = K, Rb,  $\text{NH}_4$ ) are shown in Fig. 2. It is evident that the thermal behaviour for the  $\text{NH}_4$ -compound differs from the remaining isomorphous phases.

**Table 2** Vibrational behaviour of  $\text{MH}_2(\text{IO}_3)_3$  (*M* = K,  $\text{NH}_4$ , Rb). Values in  $\text{cm}^{-1}$

$\text{KH}_2(\text{IO}_3)_3$		$\text{NH}_4\text{H}_2(\text{IO}_3)_3$		$\text{RbH}_2(\text{IO}_3)_3$		Assign.
IR	Raman	IR	Raman	IR	Raman	
		3220 br	3200 w			v N-H
		1430 m	1430 vw			v N-H
1230 w		1220 m		1220 m		$\delta$ I-O-H
1090 w		1110 w	1115 vw	1085 w		
825 sh	822 w	843 sh	823 w	843 sh	828 w	$\nu_3$ $\text{IO}_3$
790 s	801 w	790 sh?	804 w	790 sh	800 w	
755 s	759 s	765 vs	762 vs	762 vs	764 vs	$\nu_1$ $\text{IO}_3$
	741 vs		747 vs		748 vs	$2\nu_2$ $\text{IO}_3$
710 sh	685 m	710 m	687 m	710 m	689 m	v I-O...(H)
625 m	654 m	665 m	660 sh	640 m	662 m	
385 sh	372 w	375 sh	373 w	380 sh	374 w	$\nu_2$ $\text{IO}_3$
	352 w	360 sh	352 w	360 sh	350 w	
340 m	339 w	335 m	338 w	340 m	339 w	$\nu_4$ $\text{IO}_3$
	330 w		328 w		328 w	
310 m						lattice modes
	302 w		301 w		302 w	
285 sh		290 m		295 w		
	234 vw		233 vw		234 vw	
	215 vw		213 vw		212 vw	

s: strong; vs: very strong; m: medium; w: weak; vw: very weak; sh: shoulder; br: broad

### a) $\text{NH}_4\text{H}_2(\text{IO}_3)_3$

As it is observed in Fig. 2c, the DTA curve of this phase shows a small exothermic peak at  $200^\circ\text{C}$  and two well developed endothermic peaks at  $158^\circ$  and  $420^\circ\text{C}$  respectively. They are identified with two strong weight-losses on the TG curve, one located between  $155^\circ$ – $200^\circ\text{C}$  and the other between  $390^\circ$ – $420^\circ\text{C}$ . In the first one, there seems to be two successive and partially superposed processes of difficult resolution. The formation of the  $\text{NH}_4\text{IO}_3\text{I}_2\text{O}_5$  phase, suggested in

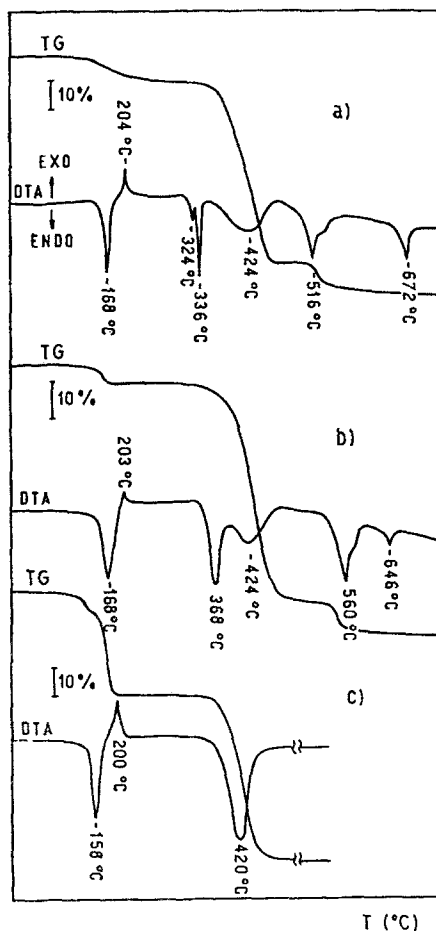
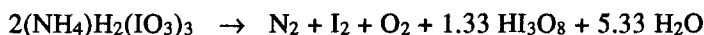


Fig. 2 TG and DTA plots of: a)  $\text{KH}_2(\text{IO}_3)_3$ , b)  $\text{RbH}_2(\text{IO}_3)_3$ , c)  $\text{NH}_4\text{H}_2(\text{IO}_3)_3$

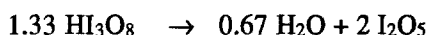
the literature [21] has not been detected and iodine is given up at  $\approx 160^\circ\text{C}$ . Likewise, IR spectra of samples heated at this temperature have not shown the typical N-H vibrations. On the other hand, the spectra of the polymeric  $\text{HI}_3\text{O}_8$  species [19, 22] have been clearly observed near  $200^\circ\text{C}$ , as an intermediate phase which easily becomes  $\text{I}_2\text{O}_5$ . The presence of  $\text{HI}_3\text{O}_8$  depends fundamentally on the heating rate and on the particle size of the sample. The small exothermic peak is associated with this formation. The second step of the thermal treatment ( $420^\circ\text{C}$ ) corresponds to the  $\text{I}_2\text{O}_5$  decomposition with the evolution of  $\text{I}_2$  and  $\text{O}_2$  [23] with a 100% weight loss. Hence, from the experimental weight-loss values, 38.5% for the first overall process and 61.5% for the second one, and with the aid of the IR

spectroscopy and XRD techniques, the degradation process can be formulated as follows:

First step: (158°–204°C):

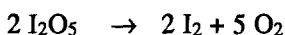


(partial weight loss: 37.6%)



(partial weight loss: 0.9%)

Second step (420°C):



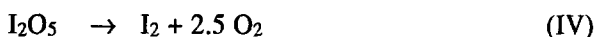
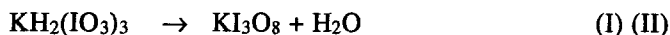
This behaviour resembles the thermal  $\text{NH}_4\text{H}(\text{IO}_3)_2$  compound [24].

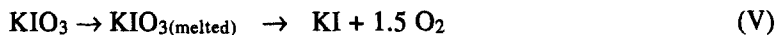
b)  $\text{MH}_2(\text{IO}_3)_3$  ( $M = \text{K}, \text{Rb}$ )

As it can be observed in Fig. 2a and b, the DTA curves of both compounds show a greater number of thermal effects in relation to the ammonium phase.

The first endothermic peaks in both compounds are attributed to the dehydration process with the subsequent rearrangement of the lattice for the formation of the polymeric  $\text{MI}_3\text{O}_8$  crystalline phase. This can be clearly identified by starting from 210°C, and its formation is surely associated to the small exothermic peak. These polymeric phases are related to  $\text{HI}_3\text{O}_8$  but this last species is more unstable [23]. Figure 3 shows a comparison of the  $\text{KI}_3\text{O}_8$ ,  $\text{RbI}_3\text{O}_8$  and  $\text{HI}_3\text{O}_8$  IR spectra, which are all intermediate phases. The characteristic stretching of the I–O–I bridges are observed in the 400–650  $\text{cm}^{-1}$ . The stretchings and bendings of the iodate groups [19] are located between 650–850 and below 400  $\text{cm}^{-1}$  respectively. The stability of the  $\text{MI}_3\text{O}_8$  remains up to 350°C approximately, and for the cation with the more polarizing power, the stability is lower. So, the decomposition process occurs at 338° and 360°C for the K and Rb compounds respectively.

The subsequent formation of the respective  $\text{MIO}_3$  and  $\text{I}_2\text{O}_5$  is clearly observed, without weight loss, at these temperatures, in agreement with the endothermic peaks. Table 2 shows the different steps of the  $\text{KH}_2(\text{IO}_3)_3$  and  $\text{RbH}_2(\text{IO}_3)_3$  thermal process which can be sustained with the aid of the XRD and IR spectroscopy. The complete and typical decomposition scheme for the potassium phase is the following:





### Conclusions

In a first place, it is important to remark that the KBr pellet technique for the IR measurements cannot be used in these systems, due to the redox reaction between the bromide and iodate acid species, situation that induces to erroneous results. For this reason, the IR previous data [12] are not reliable.

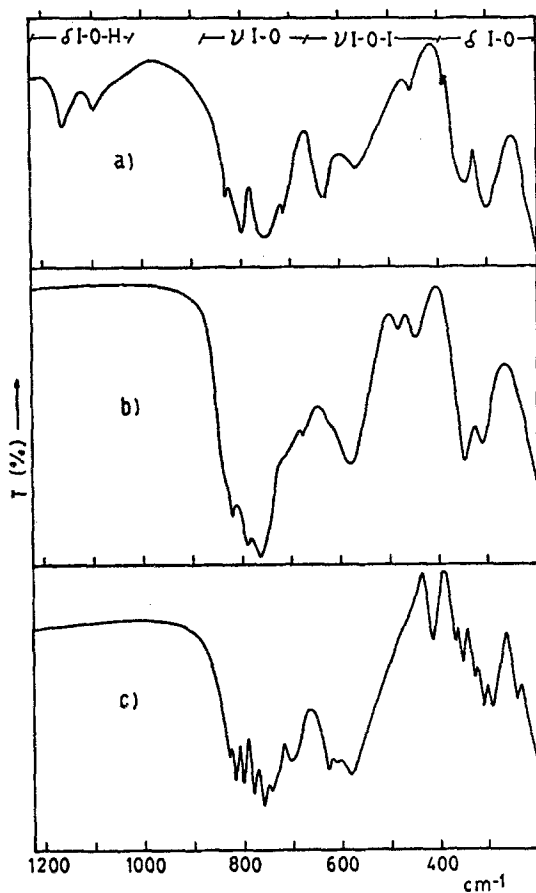


Fig. 3 IR spectra of the intermediate phases of the thermal process: a:  $\text{HI}_3\text{O}_8$ , b:  $\text{KI}_3\text{O}_8$ , c:  $\text{RbI}_3\text{O}_8$

**Table 3**  $\text{KH}_2(\text{IO}_3)_3$  and  $\text{RbH}_2(\text{IO}_3)_3$  thermal process

Type of reaction	$\text{KH}_2(\text{IO}_3)_3$							$\text{NH}_4\text{H}_2(\text{IO}_3)_3$					
	EN	EX	EN	EN	EN	EN	EN	EN	EX	EN	EN	EN	EN
$T / ^\circ\text{C}$	168	204	324	336	424	516	672	168	203	368	424	560	646
theor. weight loss / %	3.18	—	—	—	59.00	8.48	—	2.94	—	—	54.53	7.84	—
exp. weight loss / %	3.20	—	—	—	59.10	8.47	—	2.96	—	—	54.52	7.86	—
step	I	II	III	III	IV	V	VI	I	II	III	IV	V	VI

EN: endothermic, EX: exothermic

From the XRD and vibrational appreciation, the  $\text{RbH}_2(\text{IO}_3)_3$  cell dimensions as well as the I–O distances are expected to be comparable to the ammonium compound. Then a good protonic mobility can also be predicted for the Rb-phase.

On the other hand, the thermal treatment of the  $\text{NH}_4^-$  as well as K- and Rb-phases does not occur in a similar way; however, the presence of the  $[\text{I}_3\text{O}_8]^-$  polymeric and unstable species can be observed, as an intermediate phase, in all compounds, previous to the  $\text{I}_2\text{O}_5$  formation. Likewise, the thermal behaviour of the  $\text{MI}_3\text{O}_8$  ( $M = \text{K}, \text{Rb}$ ) is affected by the polarizing power of the cation. These polymeric phases are easily characterized by IR spectroscopy, presenting typical I–O–I vibrations between  $400\text{--}600\text{ cm}^{-1}$ , besides the correspondent to the I–O stretching and bending.

\* \* \*

This work was supported by CONICET (Programa QUINOR) and CICPBA.

## References

- 1 A. L. Baranov, G. O. Dobrzanski, V. V. Ilyukhin, V. S. Ryabkin, Yu. N. Sokolov, N. I. Sorokina and L. A. Shuvalov, *Krist.*, 26 (1981) 1259.
- 2 F. A. Alton and J. J. O'Connor, *Mater. Res. Bull.*, 6 (1971) 653.
- 3 T. G. Balicheva and G. Petrova, *Prob. Sourem Khim. Koord. Soedin.*, 4 (1974) 266, C. A. 82-147674 z.
- 4 V. I. Vavilin, I. F. Burshtein, B. M. Schchedrin, V. V. Ilyukhin and N. V. Belov, *Dokl. Akad. Nauk. SSSR*, 226 (1976) 1073, C. A. 84-143246 e.
- 5 A. I. Baranov, G. F. Dobrzanski, V. V. Ilyukhin, V. P. Kalinin, V. S. Ryabkin and L. A. Shuvalov, *Krist.* 24 (1979) 280.
- 6 Fu Zhengmin, Li Wenxin and Chen Liquan, *Wuli Xuebao*, 30 (1981) 1383, C. A. 226563 j.
- 7 Fu Zhengmin, Li Wenxin, Dai Jinbi and Liang Dongcai, *Wuli Xue*, Xue bav, 3 (1987) 35, C. A. 106-129711.
- 8 E. A. Soldatov, V. V. Ilyukhin, E. A. Kuzlmin and N. V. Belov, *Dokl. Akad. Nauk. SSSR*, 252 (1980) 615., C. A. 93-123992 e.

- 9 N. I. Sorokina, L. A. Muradyan, A. A. Loshmanov, L. E. Fykin, E. E. Rider, G. F. Dobrzhanskii and V. I. Simonov, *Krist.*, 29 (1984) 220.
- 10 P. Bordet, J. X. Boucherle, A. Santoro and M. Marezio, *Solid State Ionics*, 21 (1986) 243.
- 11 R. D. Shannon, *Acta Crystallogr.*, A32 (1976) 751.
- 12 N. Santha, M. Isaac, V. U. Nayar and G. Keresztury, *J. Raman Spectrosc.*, 22 (1991) 419.
- 13 E. J. Baran and P. J. Aymonino, *Spectrochim. Acta*, 24A (1968) 288.
- 14 E. J. Baran and P. J. Aymonino, *Monatsh. Chem.*, 99 (1968) 606.
- 15 K. Nakamoto, 'Infrared and Raman Spectra of Inorganic and Coordination Compounds', 3rd Ed., J. Wiley, New York 1978.
- 16 H. Siebert, 'Anwendungen der Schwingungsspektroskopie in der anorganischen Chemie' Springer-Verlag, 1966.
- 17 W. E. Dasent and T. C. Waddington, *J. Chem. Soc.*, (1960) 2429.
- 18 M. Maneva and M. Georgiev, *Spectroscopy Lett.*, 23 (1990) 831.
- 19 Th. Dupuis and J. Lecomte, *Comp. Rendus Acad. Sci. Paris*, 252 (1961) 26.
- 20 M. Maneva and M. Georgiev, *Polyhedron*, 8 (1989) 357.
- 21 A. M. Pertosyan and V. B. Gavalyan, *Zh. Neorg. Khim.*, 31 (1986) 2491.
- 22 P. M. A. Sherwood and J. J. Turner, *Spectrochim. Acta*, 26A (1970) 1975.
- 23 K. Selte and A. Kjekshus, *Acta Chem. Scand.*, 22 (1968) 3309.
- 24 C. Duval, 'Inorganic Thermogravimetric Analysis', 2nd Ed., Elsevier, 1963.

**Zusammenfassung** — Als Teil einer Studie der Eigenschaften von Feststoff-Protonenleitern wurde neben den IR- und Raman-Spektren auch das thermische Verhalten der isomorphen Verbindungen  $MH_2(IO_3)_3$  ( $M = K, Rb, NH_4$ ) untersucht. In den drei Phasen wurden mit Hilfe von TG, DTA, IR und Röntgendiffraktionsuntersuchungen detaillierte Stöchiometrien entwickelt. Es gab auch Beweise für die Bildung von polymeren  $[I_3O_8]^-$  Phasen. Ihre Stabilität steht in Verbindung mit der unterschiedlichen Polarisationsfähigkeit der H-, K- und Rb-Kationen.